JOURNAL OF MATERIALS SCIENCE 18 (1983) 3355–3362

Phase composition and structure of boride layers grown on laboratory-cast low-chromium alloys

M. CARBUCICCHIO, E. ZECCHI
Institute of Physics, University of Parma, Italy

G. PALOMBARINI, G. SAMBOGNA
Institute of Metallurgy, University of Bologna, Italy

Three Fe–C–Cr alloys containing up to 5.65 wt % Cr have been laboratory cast and homogenized, borided for 15 h at 850° C with a B_4C-base powder mixture and then characterized by using surface Mössbauer spectroscopy, X-ray diffraction, metallography and microhardness measurements. The boriding depth and the nature, disposition and relative amounts of the reaction products have been determined and discussed with regard to the chromium content in the alloys. The mechanical compactness and hardness of the innermost Fe_2B single-phase layers, which are quantitatively predominant in the boride coatings, have been related to the extent of crystallographic order.

1. Introduction

Boriding is frequently used to increase considerably the surface hardness of iron alloys obtaining, in this way, materials more suitable to resist adhesive or abrasive wear. Iron borides, in fact, are very hard but brittle compounds (Vickers hardness, HV = 13 to 24 kN mm^{-2}). Much research has been carried out on alloyed materials. In general, concern has been directed towards commercial steels, i.e. materials rather complex for the role of each alloying element to be easily pointed out. Exceptions are a few papers dealing with boriding of laboratory-cast binary [1–4] and ternary alloys [4, 5].

Because of its presence in several classes of thermochemically-treatable steels, chromium is to be considered an alloying element of particular interest for boriding. In the literature, information, to some extent contradictory, is available on the influence that chromium may exert on the boriding process and on the properties of the surface layer thus produced. In this paper, surface layers of borided Fe–C–Cr alloys containing less than 6 wt % Cr have been studied. The chromium content was selected considering that (i) the difficulties of boriding iron alloys are known to increase at higher alloying element contents [4], and (ii) in several applications, high-alloy materials could be advantageously substituted by surface-borided low-alloyed steels.

2. Experimental details

Mixtures of carburized Armco iron and pure chromium were melted in a middle-frequency induction furnace, then cast and homogenized by prolonged thermal treatments. In this way, three alloys were prepared containing 0.2 wt % C and, for the mainly alloying element, 1.26, 2.82 and 5.65 wt % Cr, respectively.

Sheets of about 25 × 15 × 1 mm^3 were surface finished with emery papers up to a 600 grit and borided for 4, 8 and 15 h at 850° C in contact with a B_4C-base (20 wt %) powder mixture containing KBF_4 (2.5%) as the activator and SiC as the diluent, following a pack-cementation procedure.

Cross-sections of treated samples were metallographically prepared, observed under optical and scanning electron microscopes and, finally, they were utilized to measure the thickness and microhardness of the boride coatings with the aid of a Vickers indenter with a 0.5 N load.

X-ray diffraction analyses were carried out

0022–2461/83 $03.00 + .12

using a X-ray generator equipped with a computer-controlled goniometer, and the Co$K\alpha$ radiation. Mössbauer measurements were performed using the experimental apparatus described elsewhere [6] and by detecting the K X-rays (6.4 keV) and the K-shell conversion electrons (7.3 keV) resonantly re-emitted by the ^{57}Fe atoms. As far as the electrons are concerned, energies in the 5.5–7.3, 6–7.3 and 6.5–7.3 keV ranges were selected. The thicknesses of the corresponding surface layers were estimated according to Krakowski and Miller [7] with a correction for the escape of detected radiation for different phases [8]. A 40 mCi ^{57}Co(Pd) source was used. The spectra were measured at room temperature and computer fitted to a series of Lorentzian lines.

3. Results

3.1. X-ray diffraction analysis

The X-ray diffraction (XRD) of as-borided 5.65 wt % Cr samples only shows resolved peaks of FeB. After surface abrasions down to ~ 20 μm in depth, the XRD patterns show, in addition, some peaks of Fe_2B (Fig. 1a). On the abraded samples, (0 0 2) preferred crystallographic orientations appear both in FeB and in Fe_2B; their intensities greatly increase near the Fe_2B/FeB (Fig. 1b) and Fe_2B/alloy interfaces.

At lower chromium contents, both FeB and Fe_2B peaks were detected from the as-borided alloys (Fig. 1c). The intensification of the (0 0 2) XRD peaks on layer-by-layer abraded samples indicates that, also for low-Cr alloys, this preferred orientation of FeB and Fe_2B crystals was increased near the FeB/Fe_2B and Fe_2B/alloy interfaces.

3.2. Surface Mössbauer measurements

Figs. 2a and b show the 6.4 keV X-ray Mössbauer spectra (estimated depth of analysis, 25–28 μm) for borided Fe–C–1.26 wt % Cr and borided Fe–C–5.65 wt % Cr alloys, respectively. For the same 5.65 wt % Cr sample, the 6–7.3 keV conversion electron spectrum (estimated depth, ~ 120 nm) is shown in Fig. 2c. All these spectra can be described in terms of various superimposed spectra:

(i) the sextet θ, which only contributes to the spectrum in Fig. 2a;

(ii) the sextets ϵ and η, which contribute to all the spectra reported in Fig. 2;

(iii) the single line and the quadrupole doublet, δ, which contribute to the spectra in Figs. 2b and c.

The analysis of their Mössbauer parameters (Table I), suggests that: sextet θ is due to Fe_2B [9], sextet η to FeB [10], and sextet ϵ to FeB_x

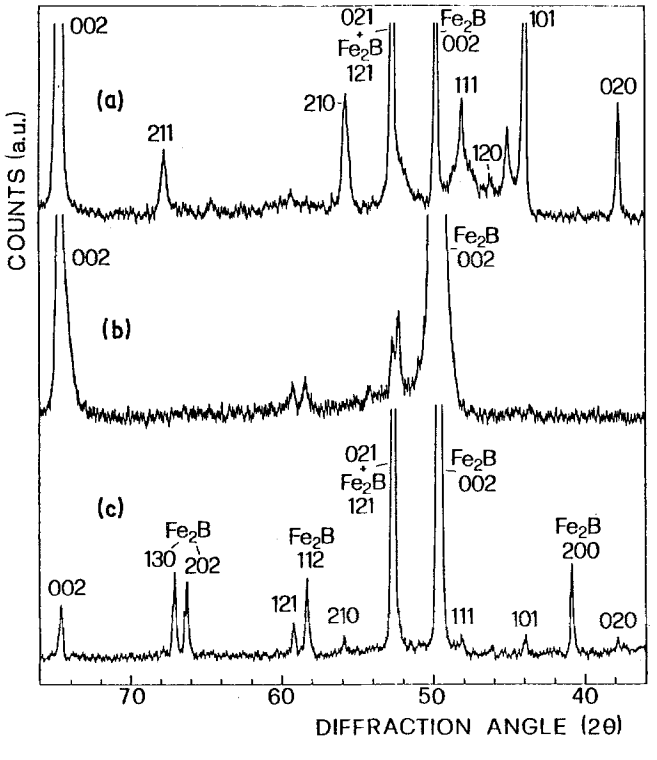

Figure 1 X-rays diffraction patterns: (a), (b) for the borided Fe–C–5.65 wt % Cr alloys, after abrasion of surface layers ~ 20 and ~ 30 μm thick, respectively; and (c) for the as-borided Fe–C–1.26 wt % Cr alloys.

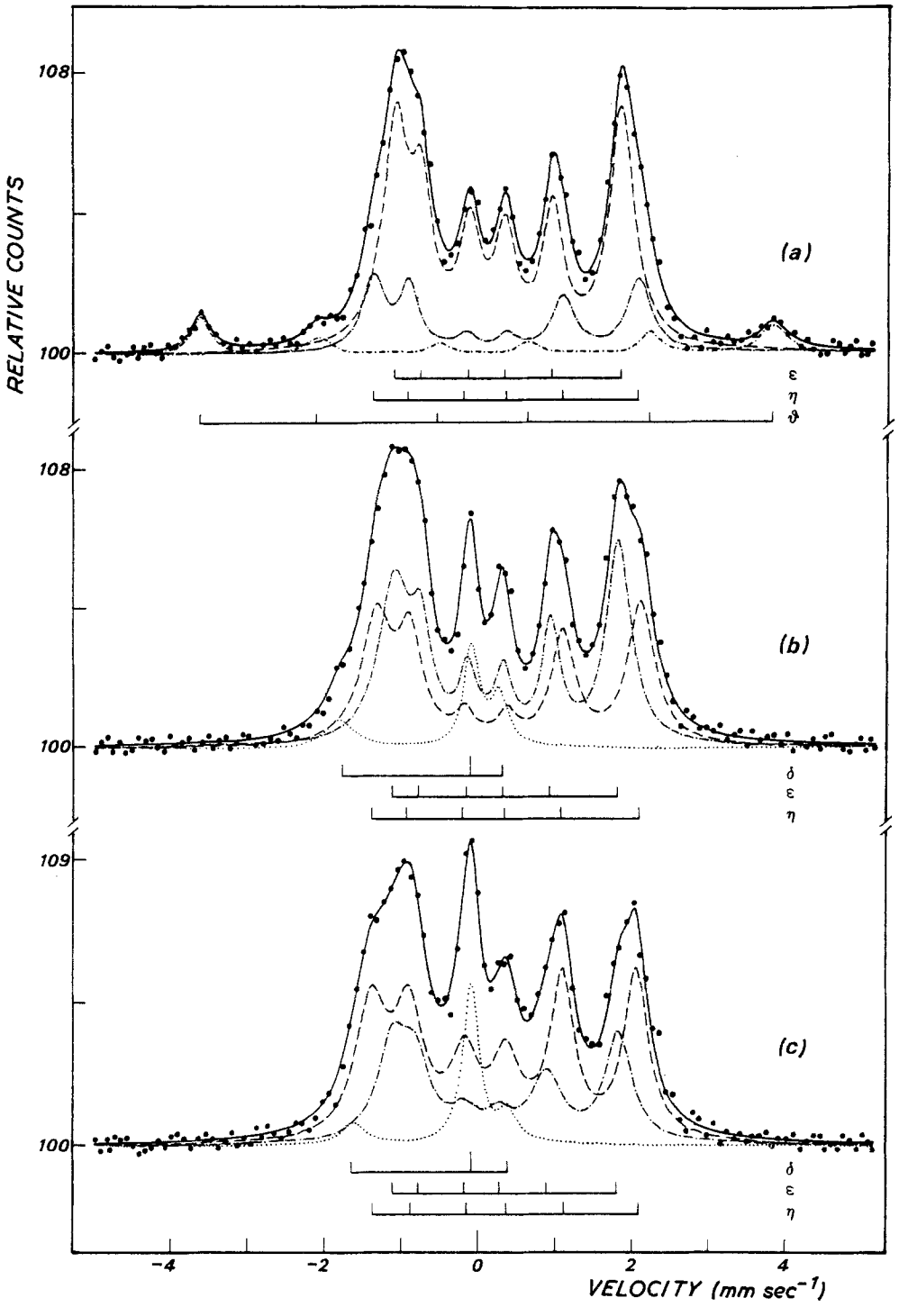

Figure 2 Room-temperature surface Mössbauer spectra, (a) for the as-borided Fe–C–1.26 wt % Cr alloys (6.4 keV X-rays); and for the as-borided Fe–C–5.65 wt % Cr alloys: (b) 6.4 keV X-rays, (c) 6–7.3 keV conversion electrons.

with $x > 1$ [5]. The single line and quadrupole doublet, δ, can be ascribed to iron in the boron solid solution, $(B, Fe)_{ss}$ [11].

The small but appreciable differences existing between the Mössbauer parameters of the spectral contributions and those reported in the literature are to be pointed out as being a reasonable consequence of the known tendency of chromium to substitute for iron in iron borides. The presence of chromium in the iron borides thermochemically

TABLE I Mössbauer parameters for laboratory-cast and borided Fe–C–Cr alloys: hyperfine magnetic fields (H_{hf}) in kOe, quadrupolar splittings (QS) and isomer shifts referred to Rh (IS) in mm sec^{-1}

Sample	Detected radiation	sextet θ			sextet η			sextet ϵ			doublet δ		single-line
		H_{hf} ± 4 (kOe)	QS ± 0.05 (mm sec^{-1})	IS ± 0.10 (mm sec^{-1})	H_{hf} ± 2 (kOe)	QS ± 0.02 (mm sec^{-1})	IS ± 0.03 (mm sec^{-1})	H_{hf} ± 2 (kOe)	QS ± 0.02 (mm sec^{-1})	IS ± 0.03 (mm sec^{-1})	QS ± 0.05 (mm sec^{-1})	IS ± 0.05 (mm sec^{-1})	IS ± 0.02 (mm sec^{-1})
Fe–C–1.26 wt % Cr	6.4 keV X-rays	233	0.05	0.10	107	0.26	0.25	91	0.28	0.26			
Fe–C–5.65 wt % Cr	6.4 keV X-rays				107	0.29	0.26	91	0.27	0.24	2.07	−0.75	−0.07
Fe–C–5.65 wt % Cr	6–7.3 keV conversion electrons				107	0.24	0.23	91	0.31	0.22	2.02	−0.65	−0.08

grown on our Cr-alloyed steels was confirmed also by analytical checks performed by an electron microprobe technique.

From the comparison between the 6.4 keV X-ray Mössbauer spectra (Figs. 2a and b), it follows that, as the chromium content increases in the base alloys,

1. the thickness of the layers containing reaction products richer in boron than Fe_2B increases (lack of sextet θ in spectrum in Fig. 2b);
2. the formation of $(B, Fe)_{ss}$ is allowed (presence of the single line and the quadrupole doublet, δ, in the spectrum in Fig. 2b and their absence in Fig. 2a);
3. the FeB/FeB_x ratio increases (as determined from area measurements). Therefore, the $(B, Fe)_{ss}$ has grown at the expense of FeB_x.

From the comparison between the conversion electron spectrum (~ 120 nm, Fig. 2c) and the 6.4 keV X-ray spectrum ($\sim 25\,\mu$m, Fig. 2b) of the same 5.65 wt % Cr borided sample, it appears that the near-surface regions contain the same products, i.e. the FeB and FeB_x Cr-containing borides and the $(B, Fe)_{ss}$ solid solution. As the external surface is approached, however, the $(B, Fe)_{ss}$ contribution to the spectra increases, while the FeB_x/FeB ratio decreases.

The 6.4 keV X-ray Mössbauer spectra for the same 5.65 wt % Cr borided sample, after cautious layer-by-layer abrasions, illustrated that (i) the $(B, Fe)_{ss}$ solid solution formed close to the external surface (lack of the single line and quadrupole doublet δ after an abrasion of a $\sim 5\,\mu$m thick surface layer), and (ii) Fe_2B formed beneath $40\,\mu$m in depth (appearance of a ferromagnetic component due to iron atoms in Fe_2B into the spectrum measured after abrasion of a further $\sim 15\,\mu$m thick layer).

3.3. Metallography

Fig. 3 shows a metallographic cross-section of a borided Fe–C–Cr alloy. Boride layers appear to be grown following an inward diffusion of a boriding species: a first reaction product, and precisely the above-mentioned Fe_2B, grew at preferred zones of the base alloy such as grain boundaries (Fig. 4) and others, assuming acicular shapes generally oriented normal to the external surfaces, i.e. along the concentration gradient of the boriding species (Fig. 5).

Because of the columnar morphology of layer-

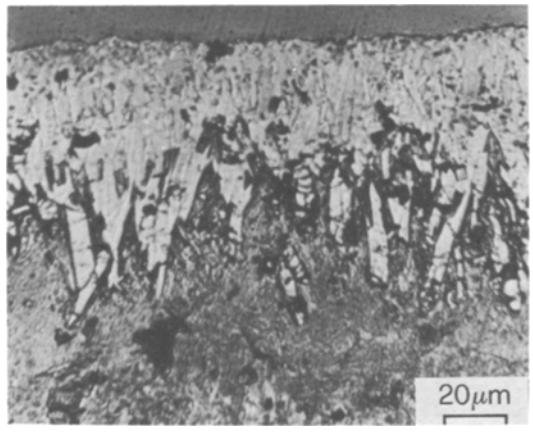

Figure 3 Optical micrograph of a cross-section of an Fe–C–1.26 wt % Cr alloy borided for 15 h at 850° C, showing a tooth-like morphology of the Fe_2B/substrate interface.

substrate interfaces, the values of boriding depth range from minima to maxima, the relative differences increasing together with the length of treatment. This tendency is shown in Fig. 6. The minima are to be considered of particular importance with regard to a possible early emerging of metal zones at the external surface, e.g. as a consequence of wear or corrosion phenomena. No appreciable difference was found in maxima and minima values for different chromium contents in the base alloys, the length of treatment being the same.

The outer part of the boride layer appears to be mechanically less compact as compared to the

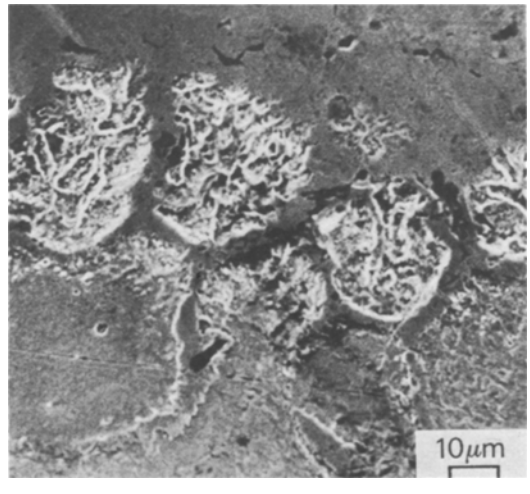

Figure 4 SEM micrograph of a cross-section of an Fe–C–5.65 wt % Cr alloy borided for 15 h at 850° C, showing a preferential growth of the boride coating at grain boundaries of the substrate.

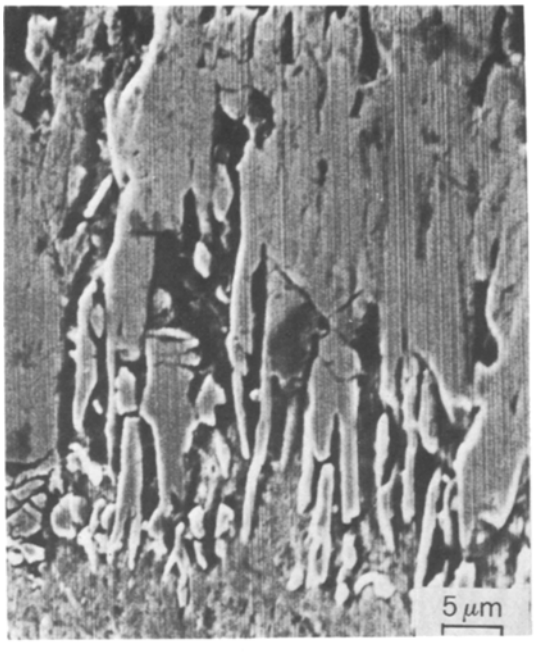

Figure 5 As in Fig. 4, showing columnar aggregates of the boride Fe_2B grown normal to the external surface.

Figure 7 SEM fractograph of the outer and mechanically less-compact part of a boride coating grown in 15 h at 850° C on an Fe–C–5.65 wt % Cr alloy.

inner part. This is confirmed by SEM fractography on borided samples V-notched and then fractured by impact loading (Figs. 7 and 8). In the more compact regions of the layers, values of hardness up to 16.5 kN mm^{-2} have been measured, the maxima being characteristic of the lowest-Cr alloy.

4. Discussion

The boride coatings grown on the Fe–C–Cr alloys are constituted by an innermost Fe_2B single-phase layer and an outermost FeB-base polyphase region. In this latter region, FeB_x with $x > 1$ was found, in addition to the boride, FeB, which is always quoted in the literature. Further investigations are

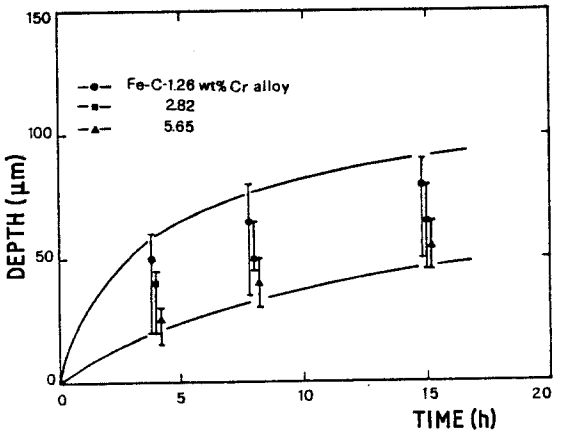

Figure 6 Maxima, minima and average metallographically-determined values of boriding depth for different lengths of treatment.

Figure 8 SEM fractograph of the inner and very compact part of the same coating shown in Fig. 7.

in progress directed towards obtaining a better understanding of FeB_x, its nature and mechanism of formation. Moreover, the presence of a $(B, Fe)_{ss}$ on the surface of the polyphase region appears to be dependent on chromium content in the base alloys. The solid solution, in fact, was absent on borided low-Cr alloys. The lowering of the FeB_x/FeB ratio at increasing content of chromium indicates that $(B, Fe)_{ss}$ has grown at the expense of FeB_x.

As the chromium content increases in the alloys, the thickness of the FeB-phase region also increases, while the total boriding depth undergoes no appreciable change. Therefore, the Fe_2B amounts correspondingly decrease in the coatings. A similar effect was recently observed for high-Cr borided steels [4].

The FeB_x/FeB ratio in the higher-Cr borided alloys decreased as the external surface was approached. This could be related to a Cr-induced embrittlement and cracking of the outer part of the coating, which is constituted by high-B products. In this way, more transformation of FeB_x into $(B, Fe)_{ss}$ was allowed along easy diffusion paths for the boriding species.

The columnar morphology of the interfaces between the base alloys and the single-phase Fe_2B layer (Fig. 3), as well as the evidence of internal boriding processes leading to acicular islands of Fe_2B oriented about normal to the external surface (Fig. 5), support the mechanism of growth previously proposed for high-purity iron boriding with crystalline boron powder [12]. In that case, only a fraction of the exposed surface reacted. Continuous layers of reactions products could not be obtained even after carburizing pure iron up to 0.3 wt % C nor after cold-rolling it up to a 22% reduction in thickness. Boriding is likely to be controlled by Fe_2B nucleation, the reaction proceding easily at the tips of Fe_2B nuclei, where particularly-high stress fields and lattice distortions are likely to be responsible for acicular and columnar growth.

5. Conclusions

The investigation on laboratory-cast alloys containing up to 5.65 wt % Cr, powder borided for 4, 8 and 15 h at 850° C, has led to the following conclusions.

1. Borided surface layers contain Fe_2B, FeB, FeB_x (with $x > 1$) and, depending on the chromium content in the base alloys, a $(B, Fe)_{ss}$ solid solution as reaction products. Fe_2B is the innermost product and it is the only one arranged as a single-phase layer. The $(B, Fe)_{ss}$ is the outermost product; it forms when the chromium contents are sufficiently high and it seems to grow at the expense of FeB_x. The concentrations of FeB and $(B, Fe)_{ss}$ increase toward the external surfaces.

2. Chromium enters iron borides substituting for a few at % Fe, modifying the relative amounts of the products at the surface of the coatings. As the chromium content increases in the alloys, the thickness of the outermost FeB-base polyphase region also increases. An opposite effect was observed with laboratory-cast Fe–C–Ni alloys, as the nickel content increased up to 8.85 wt % [5].

3. Growth of columnar aggregates of ordered crystals was allowed, following inward diffusion of boriding species along preferential paths such as grain boundaries in the alloys. Fe_2B and FeB display (0 0 2) preferred crystallographic orientations, which are particularly strong near the FeB/Fe_2B and Fe_2B/alloy interfaces. Mechanical compactness and hardness of the layers appear to be linked to the extent of crystallographic order.

Acknowledgements

This work was carried out with financial support from CNR, Italy, under "Progetto Finalizzato Metallurgia".

References

1. V. G. PERMYAKOV, I. Kh. TRUSH, V. F. LOSKUTOV, V. N. PISARENKO and Yu. E. YAKOVCHUK, *Met. Sci. Heat Treat.* **15** (1973) 1005.
2. I. Kh. TRUSH, V. G. PERMYAKOV and B. S. KIRCHEV, *ibid.* **16** (1974) 270.
3. V. G. PERMYAKOV, V. F. LOSKUTOV, V. P. BELYAEVA, V. N. PISARENKO and I. Kh. TRUSH, *Zashch. Pokrytiya Metallakh (Protective Coatings on Metals)* **9** (1975) 50.
4. P. GOEURIOT, R. FILLIT, F. THEVENOT, J. H. DRIVER and H. BRUYAS, *Mater. Sci. Eng.* **55** (1982) 9.
5. M. CARBUCICCHIO, G. MEAZZA and G. PALOMBARINI, *J. Mater. Sci.* **17** (1982) 3123.
6. M. CARBUCICCHIO, *Nucl. Instr. Meth.* **144** (1977) 225.
7. R. A. KRAKOWSKI and R. B. MILLER, *ibid.* **100** (1972) 93.
8. V. E. COSSLETT and R. N. THOMAS, *Brit. J. Appl. Phys.* **15** (1964) 883.
9. I. D. WEISMAN, L. J. SWARTZENDRUBER and L. H. BENNET, *Phys. Rev.* **177** (1969) 465.
10. H. BUNZEL, E. KREBER and U. GONSER, *J. Phys. (Paris)* **35** (1974) C6.609.

11. F. STANKE and F. PARAK, *Phys. Status Solidi* **52** (1972) 69.
12. M. CARBUCICCHIO, L. BARDANI and G. SAMBOGNA, *J. Mater. Sci.* **15** (1980) 1483.

Received 28 February
and accepted 18 March 1983